

# 1 Relevance of near-surface soil moisture vs. terrestrial water storage 2 for global vegetation functioning

3 Prajwal Khanal<sup>1,2</sup>, Anne J. Hoek Van Dijke<sup>1</sup>, Timo Schaffhauser<sup>2</sup>, Wantong Li<sup>1</sup>, Sinikka J. Paulus<sup>1,3,4</sup>,  
4 Chunhui Zhan<sup>1,5</sup>, René Orth<sup>1,4</sup>

5 <sup>1</sup>Department of Biogeochemical Integration, Max Planck Institute for Biogeochemistry, Hans-Knöll-Straße 10, 07745 Jena,  
6 Germany

7 <sup>2</sup>Chair of Hydrology and River Basin Management, Technical University of Munich, Arcisstraße 21, 80333 Munich, Germany

8 <sup>3</sup>Chair of Terrestrial Ecohydrology, University of Jena, Burgweg 11, 07749 Jena, Germany

9 <sup>4</sup>Chair of Modeling of Biogeochemical Systems, Faculty of Environment and Natural Resources, University of Freiburg,  
10 Tennenbacher Straße 4, 79106 Freiburg, Germany

11 <sup>5</sup>Chair of Land Surface-Atmosphere Interactions, Technical University of Munich, TUM School of Life Sciences  
12 Weißenstephan, 85354 Freising, Germany

13 *Correspondence to:* Prajwal Khanal (ktm.prajwalkhanal@gmail.com)

14 **Abstract.** Soil water availability is an essential prerequisite for vegetation functioning. Vegetation takes up water from varying  
15 soil depths depending on the characteristics of their rooting system and soil moisture availability across depth. The depth of  
16 vegetation water uptake is largely unknown across large spatial scales as a consequence of sparse ground measurements. At  
17 the same time, emerging satellite-derived observations of vegetation functioning, surface soil moisture and terrestrial water  
18 storage, present an opportunity to assess the depth of vegetation water uptake globally. In this study, we characterise vegetation  
19 functioning through the Near-Infrared Reflectance of Vegetation (NIRv), and compare its relation to (i) near-surface soil  
20 moisture from ESA-CCI and (ii) total water storage from GRACE at the monthly time scale during the growing season. The  
21 relationships are quantified through partial correlations to mitigate the influence of confounding factors such as energy and  
22 other water-related variables. We find that vegetation functioning is generally more strongly related to near-surface soil  
23 moisture, particularly in semi-arid regions and areas with low tree cover. In contrast, in regions with high tree cover and in  
24 arid regions, the correlation with terrestrial water storage is comparable to or even higher than with near-surface soil moisture,  
25 indicating that trees can and do make use of their deeper rooting systems to access deeper soil moisture, similar to vegetation  
26 in arid regions. At the same time we note that this comparison is hampered by different noise levels in these satellite data  
27 streams. In line with this, an attribution analysis that examines the relative importance of these soil water storages for vegetation  
28 reveals that they are controlled by (i) water availability influenced by the climate and (ii) vegetation type reflecting adaptation  
29 of ecosystems to local water resources. Next to variations in space, the vegetation water uptake depth also varies in time.  
30 During dry periods, the relative importance of terrestrial water storage increases, highlighting the relevance of deeper water  
31 resources during rain-scarce periods. Overall, the synergistic exploitation of state-of-the-art satellite data products to

32 disentangle the relevance of near-surface vs. terrestrial water storage for vegetation functioning can inform the representation  
33 of vegetation-water interactions in land surface models to support more accurate climate change projections.

## 34 **1. Introduction**

35 The regulation of water, energy, and biogeochemical cycling between land and atmosphere is primarily dependent on  
36 vegetation. In addition, global vegetation provides essential ecosystem services such as food production and uptake of some  
37 of the anthropogenic carbon dioxide emissions (Keenan and Williams, 2018). Vegetation growth depends on nutrient, water  
38 and energy availability. As a result, on a global scale, there are regions with energy or water limited vegetation functioning  
39 (Orth, 2021). In energy-limited regions, the functioning of vegetation is controlled by radiation and temperature, as they often  
40 lack sunny and warm conditions but have ample soil moisture. In contrast, soil moisture becomes critical for vegetation growth  
41 in water-limited regions. Plant photosynthesis involves opening the stomata for the uptake of CO<sub>2</sub>, while at the same time  
42 water is lost through transpiration. However, in water-limited conditions, plants can reduce the stomatal opening to avoid water  
43 loss, leading to a decrease in photosynthesis. Hence, variations in soil moisture are likely to affect vegetation functioning in  
44 water-limited conditions. Moreover, climate change has led to an expanded water limitation on vegetation (Denissen et al.,  
45 2022) and increased vegetation sensitivity to soil moisture (Li et al., 2022). For these reasons, it is essential to better understand  
46 the dependence of vegetation functioning on soil moisture to comprehend their coping mechanisms during drought to predict  
47 the future of global water, energy, and carbon cycles.

48  
49 Plants extract water from varying soil depths based on the positioning of their roots and the availability of soil moisture and  
50 nutrients. In general, the plant water uptake depth further differs spatially across different climate regimes and vegetation  
51 types, and temporally between seasons. Vegetation in arid regions is more susceptible to fluctuations in near-surface soil  
52 moisture compared to vegetation in humid regions (Xie et al., 2019). Grasses, which generally have shorter roots than trees  
53 and shrubs, are more reliant on near-surface moisture than deeper moisture (Schenk and Jackson, 2002). Further, root water  
54 uptake profiles vary within individual plant types according to above-ground biomass and age, with larger and older trees  
55 having deeper roots capable of extracting water from deeper soil layers (Schenk and Jackson, 2002; Tao et al., 2021).  
56 Additionally, within similar climate regimes, plant water uptake varies across topographic positions. Upland and lowland roots  
57 tend to be shallower, making vegetation more reliant on near-surface soil moisture, while roots go deeper in steep terrain  
58 between these landscapes to access both surface and deep moisture (Fan et al., 2017).

59  
60 Though spatial variations of plant water uptake depths across vegetation types and climate regimes, and temporal shift during  
61 dry-months, are widely studied at point scale, inadequate deep soil moisture records pose a major obstacle to study vegetation  
62 root water uptake at a global scale. Microwave remote sensing allows to infer near-surface soil moisture dynamics globally..  
63 While microwaves penetrate only the top few centimeters and do not cover the entire soil moisture profile, they represent

64 larger depths of moisture variation, providing valuable insights into root zone soil moisture (Feldman et al., 2023) .Land  
65 surface models provide an alternative source of global soil moisture data across depths, but they are subject to uncertainties  
66 arising from meteorological data, inaccurate knowledge of soil and vegetation characteristics, and the representation of  
67 complex processes such as photosynthesis, infiltration, and evaporation (Koster et al., 2009; Seneviratne et al., 2010). Hence,  
68 some studies have employed reanalysis-based soil moisture estimates, to investigate the relationship between vegetation and  
69 soil moisture at the global scale ((Li et al., 2021; Miguez-Macho and Fan, 2021); but those are likely to be impacted by model  
70 assumptions affecting soil moisture dynamics, particularly for deeper layers where less observational constraints are available.  
71 Thus, studying vegetation interactions with the entire water column, including near-surface and deep soil moisture, at a global  
72 scale using exclusively observation-based dataset is imperative to enhance the understanding of relevance of near-surface and  
73 deep soil moisture for vegetation functioning.

74

75 The Gravity Recovery and Climate Experiment (GRACE) satellite mission, launched in 2002, provides total water storage  
76 (TWS) anomalies observations at the global scale. The TWS captures not only soil water but also snow and ice, canopy water,  
77 surface water and groundwater. Its depth of representation is therefore difficult to physically quantify, and that is why we  
78 studies TWS anomalies. Nevertheless, they seem to be related to variations of overall water availability (near-surface + deep  
79 soil moisture) for vegetation (Yang et al., 2014). The inter-annual carbon dioxide growth rate in the atmosphere, for example,  
80 has been found to be well correlated with the total water storage anomalies on a global scale, indicating the relevance of total  
81 water column for vegetation functioning (Humphrey et al., 2018). In this study, we assume that TWS anomalies can be used  
82 to estimate the variation of overall water availability (near-surface + deep soil moisture) for vegetation under (i) snow-free  
83 conditions, and assuming that (ii) water storage variations in lakes or groundwater are negligible at the monthly time scale,  
84 (iii) and canopy water storage is much smaller than soil water storage and hence also negligible. This study focuses on  
85 understanding the relevance of near-surface vs. total water storage for vegetation functioning on a global scale using  
86 observation-based datasets, thereby inferring vegetation's large-scale water uptake depth from observation-based datasets. For  
87 this purpose, we utilise TWS and near-surface soil moisture and correlate them with vegetation functioning, represented by  
88 Near-Infrared Reflectance of Vegetation (NIRv). In particular, we analyse (1) what is the relevance of near-surface soil  
89 moisture vs. the terrestrial water storage for vegetation functioning?, (2) how does the importance of near-surface soil moisture  
90 vs. terrestrial water storage change during dry months? and (3) how do climatic, vegetation, and topographic characteristics  
91 explain the variability in the relevance of near-surface vs. terrestrial water storage for vegetation functioning?

## 92 **2. Data and Methodology**

93 **Table 1: Table summarising all the datasets.**

<b>Datasets</b>	<b>Variables</b>	<b>Source</b>	<b>Spatial Resolution</b>	<b>Temporal Resolution</b>	<b>Temporal Coverage</b>	<b>References</b>
<b>Vegetation Functioning</b>	Near Infrared Reflectance of Vegetation (NIRv)	MODIS/MOD13C1 v061	0.05 degree	16 daily	2000 - present	(Badgley et al., 2017)
	Solar Induced Chlorophyll Fluorescence (SIF)	GOME-2	0.5 degree	16 daily	2007 - 2018	(Köhler et al., 2015)
<b>Soil Water Storage</b>	Near-surface soil moisture (SSM)	ESA-CCI v04.4	0.25 degree	Daily	1978 - 2022	(Dorigo et al., 2017)
	Total Water Storage (TWS) Anomalies	GRACE	0.5 degree	Monthly	2002 - present	(Landerer and Swenson, 2012)
<b>Meteorological</b>	Air Temperature (T <sub>a</sub> )	ERA-5	0.25 degree	Hourly	1940 - present	(Hersbach et al., 2020)
	Precipitation (P)					
	Net Radiation (R <sub>n</sub> )					
	Dew point Temperature (T <sub>d</sub> )					
<b>Climatological</b>	Aridity Index	Global Aridity Index and Potential Evapotranspiration Database - Version 3	30 arc seconds	Static	1970-2000	(Zomer et al., 2022)

<b>Vegetation and Land cover class</b>	Tree cover fraction	VFC5KYR	0.05 degree		1982 - 2016	(Hansen, Matthew and Song, Xiao-Peng, 2018)
	Land cover data	ESA-CCI	300 m	Yearly	1992 - 2018	ESA. Land Cover CCI Product User Guide Version 2. Tech. Rep. (2017)
<b>Topographical data</b>	Elevation	Earthenv	1 km	Static		(Amatulli et al., 2018)
	Slope					
<b>Soil data</b>	Fraction of sand	FAO	0.05 degree	Static		(Reynolds et al., 2000)
	Fraction of clay					
<b>Irrigation</b>	Percentage of Irrigated area	HID	5 arcmin	Yearly	1990 - 2005	(Siebert et al., 2015)

94

## 95 **2.1 Data**

### 96 **2.1.1 Vegetation Functioning:**

97 In our study, vegetation functioning is characterised by satellite measurements of Near-Infrared Reflectance of vegetation  
98 (NIRv) and Solar Induced Fluorescence (SIF) (**Table 1**). NIRv is the product of near-infrared reflectance and the normalised  
99 difference vegetation index (NDVI) and represents the vegetation structure and vegetation greenness (Badgley et al., 2017).  
100 The NIRv data is available at a high spatial resolution of 0.05°, and the original 16-day data was aggregated to the monthly  
101 NIRv data. SIF is directly related to the photosynthetic activity of plants because the excess energy from sunlight, that triggers  
102 the light reaction during photosynthesis, is dissipated by leaf as chlorophyll fluorescence (Mohammed et al., 2019). SIF data  
103 is derived from the Global Ozone Monitoring Experiment (GOME-2), because GOME-2 provides relatively reliable data over  
104 a long period (2007-2018). The 0.5° spatial and 16-day temporal resolution SIF data is processed into monthly data as described  
105 by (Köhler et al., 2015).

106

107 The high spatial resolution of NIRv allows for a detailed study of the correlation of vegetation functioning with soil water  
108 availability. Therefore, we performed the main analyses using NIRv data. However, SIF is more sensitive to drought stress  
109 than NIRv (Qiu et al., 2022). Therefore, we perform additional analyses with SIF to show that the relationships hold for a  
110 different and more direct indicator of vegetation functioning.

### 111 **2.1.2 Soil Water Storage**

112 This study includes two different measures of soil water availability. The near-surface soil moisture (SSM) provides an  
113 estimate of water availability in the top layer of the soil, while the Terrestrial Water Storage (TWS) Anomaly provides an  
114 estimate of the overall water column of the soil. The SSM data is derived from the European Space Agency (ESA) Climate  
115 Change Initiative Program (CCI), which combines active and passive satellite microwave measurements to provide reliable  
116 estimates of SSM (Dorigo et al., 2017). The ESA CCI soil moisture data, at a daily temporal resolution, was aggregated to  
117 monthly temporal resolution. The TWS Anomaly data is derived from the GRACE mission, which measures changes in the  
118 Earth's gravity field (Landerer and Swenson, 2012). Here, we use the JPL-Mascons product of TWS Anomalies which is  
119 available at a 0.5° spatial and monthly temporal resolution (Watkins et al., 2015)

### 120 **2.1.3 Meteorological Data**

121 Employed climate variables include monthly air temperature ( $T_a$ ), 2m dew point temperature ( $T_d$ ), precipitation (P), and net  
122 radiation ( $R_n$ ) from the ERA5 reanalysis products at a 0.25° spatial resolution. The vapor pressure deficit (vpd) is calculated  
123 from  $T_a$  and  $T_d$ . Further, the aridity index is calculated from the ratio between the long-term mean  $R_n$  ( $\text{mm y}^{-1}$ ) ( $1 \text{ MJ/sq.m/day}$   
124  $= 0.408 \text{ mm/day}$ ) and P ( $\text{mm y}^{-1}$ ) for each grid cell (Budyko, 1974). We opted for this formulation as it offers a direct estimation  
125 of aridity and water (energy) constraints on vegetation. This eliminates the necessity to navigate through various formulations  
126 utilized for calculating potential evapotranspiration. However, we conducted additional validations of our results using the  
127 Global Aridity Index dataset (Zomer et al., 2022) based upon the FAO Penman-Monteith Reference Evapotranspiration  
128 equation. The use of the Global Aridity Index did not change the results of our study (**Section 3.4**). In addition, the mean and  
129 standard deviation of the climate variables are calculated and incorporated in the attribution analysis (**Section 2.2.3**).

### 130 **2.1.4 Vegetation, soil, and topography data**

131 To evaluate the resulting correlation of vegetation functioning and water storages with respect to vegetation characteristics,  
132 we employ the tree cover fraction data from the AVHRR vegetation continuous fields products (VCF5KYR,  
133 <https://lpdaac.usgs.gov/products/vcf5kyrv001/>) (Hansen, Matthew and Song, Xiao-Peng, 2018). For this purpose, the mean  
134 of tree cover fraction for the years between 2007 and 2016 is calculated.

135 Topographical variables such as elevation and slope are incorporated along with other meteorological variables to determine  
136 the relative contribution of different variables to the correlation between vegetation functioning and water storage. Topographic  
137 data at a 5 km resolution were downloaded from the EarthEnv. These data are calculated based on the 250 m GMTED dataset

138 and compared against the 90 m SRTM 4.1 dev dataset. The data were resampled to a coarser resolution of 5 km using various  
139 aggregation techniques, details of which are in (Amatulli et al., 2018). Furthermore, for each grid cell, the fraction of sand and  
140 clay in soil (Reynolds et al., 2000) along with the percentage of irrigated area (Siebert et al., 2015) were considered in  
141 attribution analysis.

142

## 143 **2.2 Methodology**

### 144 **2.2.1 Data pre-processing**

145 A flowchart of the data pre-processing and analyses is presented in **Figure S1**. The time period of analysis is from 2007 to  
146 2018 constrained by the concurrent availability of all involved datasets. All the analyses were performed in monthly temporal  
147 resolution and at 0.05° spatial resolution (for NIRv) and 0.5° spatial resolution (for SIF). The SSM and TWS data were initially  
148 available at 0.25° and 0.5° resolution, but were disaggregated or aggregated to 0.05° or 0.5° degrees, depending on the spatial  
149 resolution of the analysis performed, based on the assumption that the soil water storage anomalies are representative over  
150 larger areas. Also, the meteorological data and vegetation, soil, and topographic data were resampled into the same resolution.  
151 After aggregating all the datasets to 0.05° resolution, the monthly anomalies were calculated by subtracting the long term mean  
152 monthly cycle and by removing linear trends. A SIF threshold was applied in each grid cell to filter out non-growing season  
153 data. For this purpose, we filtered out all the months from 2007-2018 when the mean-monthly SIF value was below the  
154 threshold of 0.2 mW/m<sup>2</sup>/sr/nm. We apply an additional temperature threshold ( $T_a > 5^\circ\text{C}$ ) to remove the months with frozen  
155 soil and snow cover, similar to (Li et al., 2021). Last, all months with missing soil water storage or vegetation functioning  
156 records were excluded.

### 157 **2.2.2 Calculate the relevance of near-surface (SSM) soil moisture and terrestrial water storage (TWS) for vegetation** 158 **functioning**

159 We calculated the Spearman correlation between vegetation functioning (NIRv) and soil water storages (SSM and TWS) for  
160 each grid cell during growing season months when observations for at least 40 months were available. The cutoff of 40 months  
161 was implemented to guarantee a substantial number of observations for growing-season months in each grid cell. This  
162 consideration assumes that the minimum number of growing-season months varies from 3 to 4 months per year globally. In  
163 addition to soil moisture, also air temperature ( $T_a$ ) and net radiation ( $R_n$ ) affect the vegetation functioning. Moreover, SSM  
164 (soil moisture) and TWS (total water storage) demonstrate a notable correlation, as illustrated in **Figure S2**, signifying the  
165 presence of mutual information. To exclusively examine the individual impacts of each water storage variable on vegetation  
166 functioning and disentangle mutual information from other water variables, we accounted for confounding effects. This  
167 entailed computing the partial correlation between NIRv and water storages (SSM or TWS), while controlling for  $T_a$ ,  $R_n$ , and  
168 the other water storage variable (TWS or SSM). Since we focus on understanding the role of soil moisture on vegetation  
169 functioning, which is primarily critical in water-limited conditions, we removed the grids cells with negative partial

170 correlations from our analysis. Such negative partial correlations may hint at vegetation's converse effect on soil moisture  
171 (when increasing vegetation activity depletes the soil moisture) and a negative correlation could occur in the grid cells where  
172 water limits vegetation productivity through oxygen limitation (Ohta et al., 2014).

173  
174 It is important to note that we chose not to apply a significance criterion in analyzing the partial correlation between NIRv and  
175 water storages. When controlling for both water storage (TWS or SSM) and energy variables (Ta and Rn) in the partial  
176 correlation (NIRv~SSM or TWS), a limited number of grid cells demonstrate significant correlation globally, given the high  
177 correlation between SSM and TWS (Figure S2). This poses challenges for drawing global inferences on vegetation water  
178 uptake. However, our overarching goal is to discern variations in the partial correlation of NIRv with water storages across  
179 differing climate-vegetation gradients and how it changes from the growing season to dry months, rather than confirming  
180 specific statistical thresholds. For this, we want to maintain a sufficient amount of grid cells necessary for making global  
181 inferences. However, to ensure that our results are not affected by the significance criterion, we conducted additional analyses  
182 considering only grid cells with a significant partial correlation (though a very small number compared to the total grid cells  
183 available for each AI-TC class globally), as described in section 3.4.

184  
185 The impact of all pre-processing steps on the number of grid cells included in this study is illustrated in Figure S3. Generally,  
186 our filtering procedures enable us to concentrate primarily on water-limited regions, as they effectively remove a substantial  
187 number of grid cells from the wet regions globally.

188 To analyse how the importance of SSM and TWS changes during dry months, we specifically selected the months characterized  
189 by the lowest 10% SSM for each grid cell, representing the driest conditions within the growing-season months. The partial  
190 correlations between NIRv and water storages,  $r(\text{NIRv} \sim \text{SSM})$  and  $r(\text{NIRv} \sim \text{TWS})$  were calculated separately for dry months.  
191 To focus on vegetation response to similar extent of dryness spatially, only grid cells with greater than 100 monthly  
192 observations were considered for the dry months analysis. In addition, only the grid cells which had positive partial correlation  
193 in growing season months were included for the dry months analysis.

194  
195 After computing the partial correlations, we grouped the grid cells by aridity and tree cover classes, which allowed us to  
196 analyse the evolution of correlations and the difference between the partial correlation across aridity-tree cover classes.  
197 Afterwards, we employed bootstrapping with 1000 repetitions to compute the bootstrap means and confidence interval using  
198 a full bootstrapping methodology (resampling with replacement from the original data) for each aridity-tree cover class with  
199 sufficient number of observations for both growing season and dry months. .

200  
201 Moreover, to test the robustness of the results, we did additional partial correlation analyses, for which we correlated the SIF  
202 (instead of NIRv) with SSM and TWS. The analyses with SIF were performed at a spatial resolution of  $0.5^\circ$ , at which SIF data  
203 was available.



### 204 2.2.3 Attribution Analysis

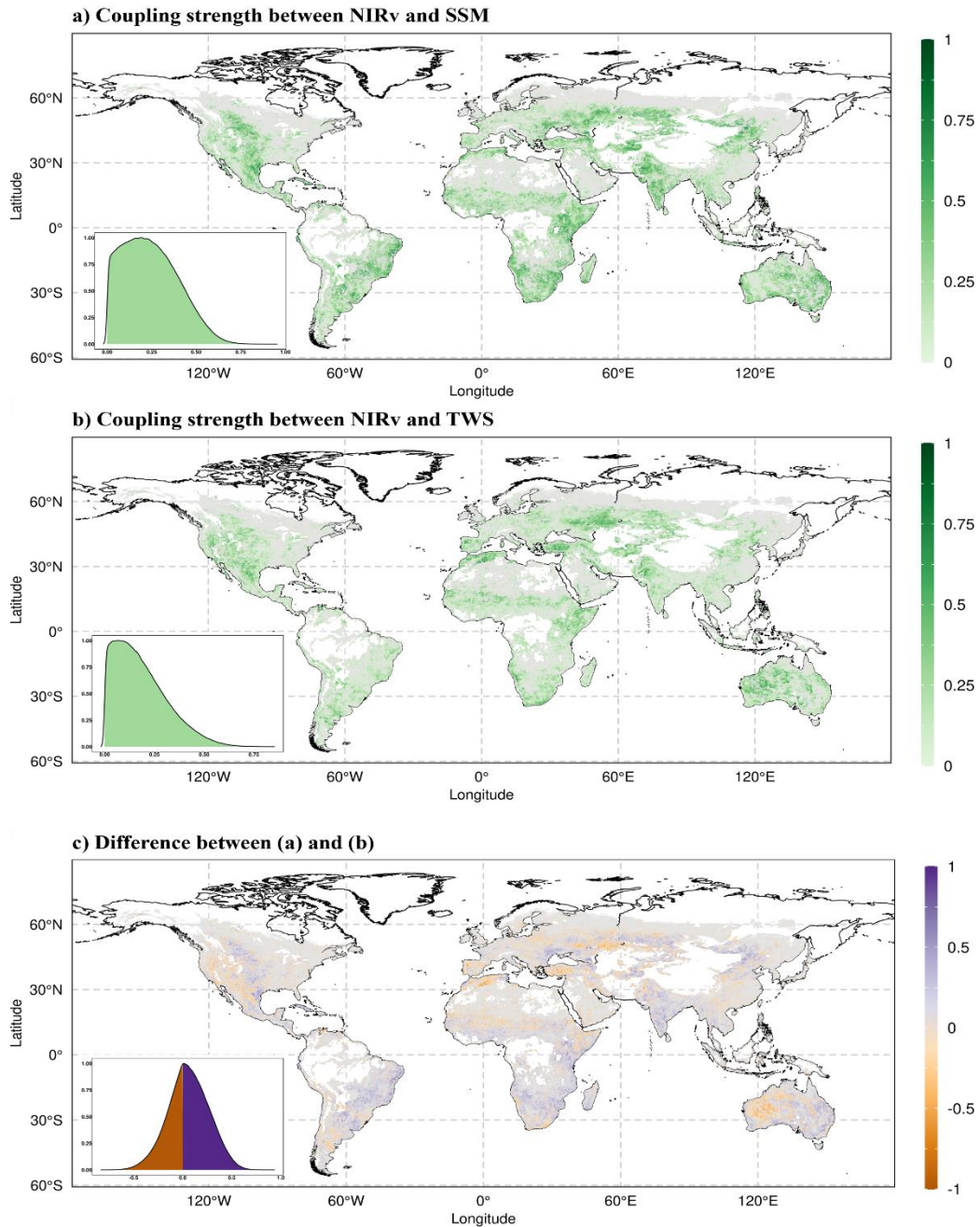
205 We used a random forest model to understand the spatial variability in the relevance of SSM versus TWS for NIRv. Random  
206 forest is a nonparametric based regression algorithm which does not require any statistical assumptions on the predictor and  
207 target variables which makes it particularly useful for detecting the nonlinear relationship (Breiman, 2001). Given potential  
208 nonlinear impacts of various factors (climate, soil types, vegetation) on the relationship between moisture storages and  
209 vegetation functioning, this study employed the random forest method to assess the relative contributions of these variables.

210

211 In our study, 15 predictors were included in the random forest model based on their potential physical relevance to the target  
212 variable, which is the difference in correlation between SSM and TWS with NIRv in growing season months. These predictors  
213 included mean and standard deviation of climate variables ( $T_a$ ,  $R_n$ , P and vpd), aridity index, topographical variables (elevation  
214 and slope), vegetation variable (tree cover), soil-related variables (fraction of clay and sand), and percentage of irrigated areas  
215 for each grid cell. We calculated the mean and standard deviation of the climate variables only during the growing-season  
216 months, as determined for the subsequent partial correlation analysis.. Furthermore, only the grid cells exhibiting positive  
217 partial correlation between NIRv and SSM as well as NIRv and TWS during growing season-months were included in the  
218 random forest analysis. For training a random forest model, we used the “xgboost” package in R (Chen and Guestrin, 2016).

219

220 We further incorporate SHAP (SHapley Additive exPlanations) values for interpreting the predictions of the random forest  
221 model (Lundberg et al., 2020). The SHAP value for a feature is the average difference in prediction of the model when that  
222 feature is included compared to when it is excluded, over all possible combinations of features. By calculating SHAP values  
223 for each feature in the model, we identified which features were most important in explaining the spatial variability in the  
224 relevance of SSM versus TWS. For calculating the SHAP values, we employed “SHAPforxgboost” package in R.



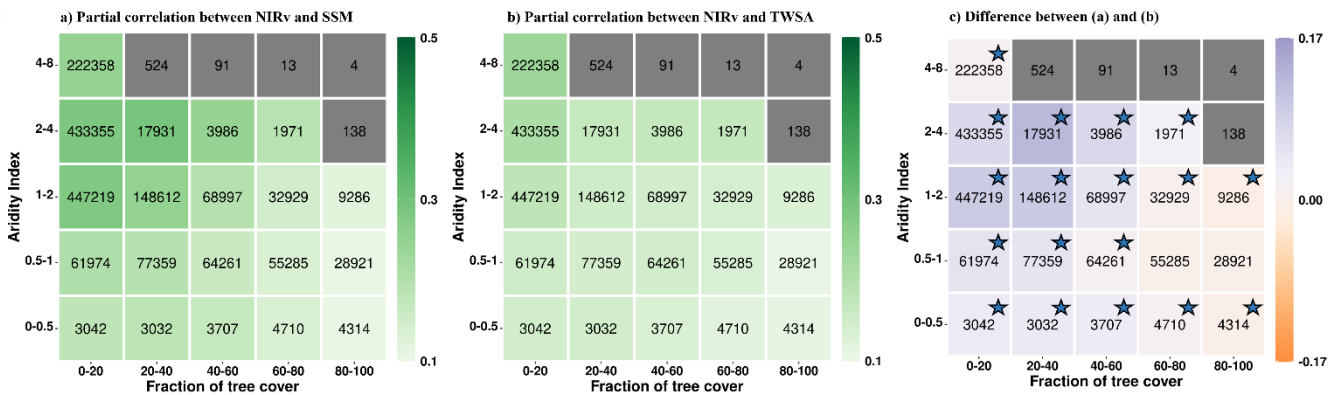
230 (c) Difference between (a) and (b). The purple colour in (c) indicates the greater partial correlation of NIRv with SSM compared to  
 231 the partial correlation of NIRv with TWS while orange colour indicates the opposite. Grid cells with positive relationships for both  
 232 correlations (a) and (b) are shown in (c) with blueish and orange colours. Light grey colour indicates negative partial correlations  
 233 between NIRv and water storage. The absence of color within the land boundary signifies inadequate observational data for precise  
 234 computation of the partial correlation. Each inset in the respective maps illustrates the probability distribution function (pdf) of the  
 235 correlations.

236 The partial correlation of NIRv with near-surface soil moisture varies globally during growing-season months (**Figure 1a**).  
 237 NIRv demonstrates stronger correlation with near-surface soil moisture within semi-arid climates, Central North America,  
 238 South America, regions in South Africa and Australia. The correlation is stronger in Southern Europe and the Mediterranean  
 239 region compared to central and Northern Europe. The correlation gradient from the hot and dry Mediterranean region to wet  
 240 and cold Northern Europe corresponds to the gradient of water-limited ecosystems to energy-limited ecosystems obtained in  
 241 other studies (Denissen et al., 2022; Teuling et al., 2009).

242  
 243 The global correlation of NIRv with TWS follows a similar pattern as with SSM (**Figure 1b**) in growing-season months. The  
 244 correlation of NIRv with TWS is higher in drier central northern America and Australia compared to other regions. The  
 245 similarities in the correlation of NIRv with SSM and TWS are expected because the monthly anomalies of SSM and TWS are  
 246 highly correlated during growing season months in most of our study area (**Figure S2**).

247  
 248 The difference between the partial correlation of NIRv with SSM and TWS (**Figure 1c**) indicates that the NIRv correlates  
 249 stronger with TWS in Western America, Southern Europe, and arid regions of Australia compared to other regions globally  
 250 during growing-season months. In South America and Southern Africa, however, the NIRv shows a stronger correlation with  
 251 SSM. Although we control for the effect of soil water storage (SSM or TWS) when computing partial correlation to discern  
 252 the relative importance for vegetation, it should be noted that the varying noise levels inherent in these datasets might impact  
 253 our results.

254  
 255



256

257 **Figure 2: Summarising the coupling strengths of vegetation functioning (NIRv) with (a) near-surface soil moisture (SSM) and (b)**  
258 **terrestrial water storage (TWS) in the growing season-months across climate (aridity index) and vegetation regimes (fraction of tree**  
259 **cover). (c) shows the difference between (a) and (b). Numbers within the boxes denote the number of grid cells for each aridity-tree**  
260 **cover class. Aridity-tree cover classes containing less than 1000 grid cells are shown in grey. The color bar denotes the mean partial**  
261 **correlation for each class, computed from bootstrapping. The asterisk in figure (c) signifies that the 95% confidence interval (lower**  
262 **and upper) shares the consistent sign (+/-) in the difference of partial correlation. Only grid cells with positive partial correlation**  
263 **are considered.**

264

265 Next, we analyse the partial correlation between NIRv and soil water storages across different aridity and tree cover fraction  
266 classes during growing season months. For this, we group the grid cells into different aridity and tree cover fraction classes  
267 and then do bootstrapping to compute mean partial correlation and the 95 percent confidence intervals for each class with more  
268 than 1000 grid cells. We find that the partial correlation of NIRv with SSM (**Figure 2a**) increases with increasing aridity for  
269 aridity index (0-4). This can be attributed to the intensification of water stress on vegetation under increasingly arid conditions,  
270 resulting in a stronger correlation between NIRv and SSM. However, for a further increase in aridity (4-8), the strength of the  
271 correlation of NIRv with SSM declines. This is due to a low soil moisture availability and low temporal variability under  
272 extremely arid conditions (Figure S4). The pattern of increasing correlation along aridity index is also observed in the partial  
273 correlation between NIRv and TWS. (**Figure 2b**).

274

275 Furthermore, the correlation of NIRv with SSM decreases for higher tree cover fractions (**Figure 2a**). However, such a gradient  
276 along tree cover fraction is less pronounced in the partial correlation of the NIRv with TWS (**Figure 2b**). This overall depicts  
277 that the coupling of vegetation functioning with SSM is generally higher for non-forested areas compared to forested areas  
278 while this gradient is less pronounced in the case of TWS.

279

280 Though the difference in inherent noise levels associated with SSM and TWS impacts partial correlation analysis, we can  
281 compare the evolution of the gradient along tree cover or aridity index and assert how the relevance of SSM and TWS changes  
282 with varying tree cover or aridity index, assuming that the noise levels are similar across varying AI-TC classes. Taking this  
283 into account, we find that NIRv correlates more strongly with near-surface soil moisture compared to terrestrial water storage  
284 in semi-arid regions with low tree cover (**Figure 2c**), suggesting that the vegetation preferentially takes up water from SSM  
285 whenever available to meet its transpiration demand. This might be due to lower energy expenditure on root water uptake,  
286 abundant nutrients and reduced chance of root water logging in the near-surface soil moisture (Feldman et al., 2023; Schenk  
287 and Jackson, 2002; Tao et al., 2021). Conversely, the correlation between the NIRv and TWS in arid areas (AI 4-8) and regions  
288 with a high fraction of tree cover is equivalent to or greater than that of SSM, suggesting that trees can utilise their extensive  
289 root systems to access deeper soil moisture, as observed in arid vegetation. This is consistent with previous studies reporting  
290 that the vegetation dependence on sub-surface soil moisture is higher in arid and seasonal-arid climates (Miguez-Macho and

291 Fan, 2021). However, in certain regions with higher tree cover in humid areas, specifically with AI 0.5-1, such conclusions  
 292 cannot be confidently drawn statistically. The reason is that the confidence intervals for the difference in partial correlation of  
 293 NIRv with SSM and TWS fluctuate between positive (indicating greater relevance of SSM) and negative (indicating greater  
 294 relevance of TWS) values (**Figure 2c**).

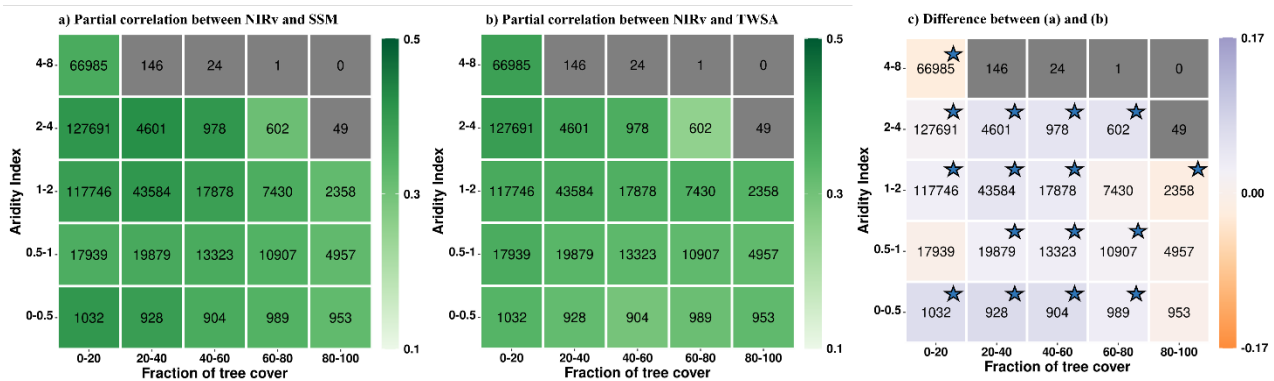
295  
 296 Note that while our analysis focuses on regions with water-controlled vegetation as denoted by positive correlations between  
 297 NIRv and the considered soil water storages, some of these grid cells are located in comparatively wet climate regimes with  
 298 aridity index values between 0 and 1 (**Figure 2**). This highlights the relevance of non-climatic factors such as soil and  
 299 vegetation types or topography in determining vegetation-water relationships in addition to the climate regime. Next to this,  
 300 in **Figure 2c** it seems that the relevance of terrestrial water storage is comparatively higher in wet climate (aridity 0.5-1) than  
 301 in transitional climate regimes (aridity 1-2) as shown with the smaller correlation differences. This, however, is probably not  
 302 the case and simply a reflection of reduced variability in surface soil moisture (**Figure S4**).

303

### 304 3.2 Coupling of vegetation functioning with surface soil moisture and total water storage in dry months

305 The correlation between NIRv and soil water storage increases during dry months (**Figure 3a,b**) compared to growing season  
 306 months (**Figure 2a,b**). This increase is consistent for both SSM and TWS and across all tree cover fractions and aridity classes.  
 307 This is because the water limitation on vegetation increases in dry months and so does the vegetation's sensitivity to the  
 308 moisture. During the dry months, the correlation with near-surface soil moisture tends to rise, but the correlation with terrestrial  
 309 water storage increases even more significantly (**Figure 3c**). This indicates the relevance of deeper water resources during  
 310 periods of scarce rainfall. The partial correlation maps (**Figure S5**) also reveal that NIRv's correlation with TWS increases  
 311 more than its correlation with SSM for most grid cells.

312



313

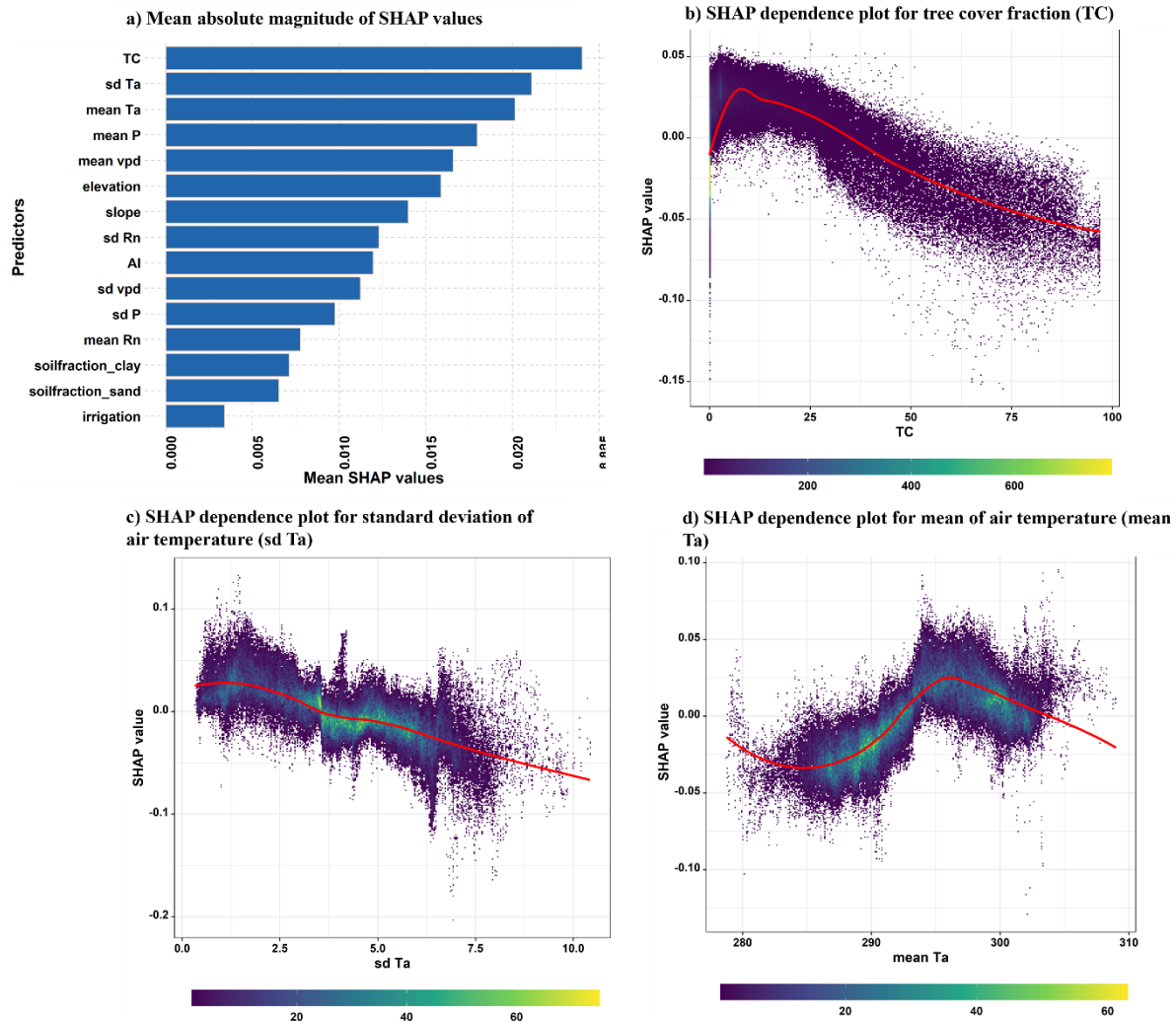
314 **Figure 3: Summarising the coupling strengths of vegetation functioning (NIRv) with (a) near-surface soil moisture (SSM) and (b)**  
 315 **terrestrial water storage (TWS) in the 10% driest months in each grid-cell across climate (aridity index) and vegetation regimes**  
 316 **(fraction of tree cover). (c) shows the difference between (a) and (b). Numbers within the boxes denote the number of grid cells for**

317 each aridity-tree cover class. Aridity-tree cover classes containing less than 1000 grid cells are shown in grey. The color bar denotes  
318 the mean partial correlation for each class, computed from bootstrapping. The asterisk in figure (c) signifies that the 95% confidence  
319 interval (lower and upper) shares the consistent sign (+/-) in the difference of partial correlation. Only grid cells with positive partial  
320 correlation are considered.

321 During dry months, the number of analysed grid cells (**Figure 3**) is lower compared to all growing season months (**Figure 2**).  
322 We performed a reanalysis of the correlation patterns within aridity-tree cover classes by selecting only those grid cells that  
323 displayed positive partial correlation between NIRv and soil water storages during both the dry months and the growing season  
324 months. The results demonstrate that the previously observed patterns remain valid, thereby eliminating the impact of the  
325 differing numbers of grid cells analysed. (**Figure S6**.

326

### 3.3 Climate, vegetation, and topographic controls on the relevance of surface soil moisture vs. total water storage on vegetation



329

330 **Figure 4: (a) Global feature importance based on the mean absolute magnitude of the SHAP values. The higher the mean SHAP**  
 331 **values, the greater the predictor’s relevance. (b-d) Evaluation of SHAP values (=contributions to the correlation difference**  
 332 **illustrated in Figure 1c) against predictor values for the 3 most relevant predictors tree cover fraction (TC), variability of**  
 333 **temperature (sd  $T_a$ ) and mean temperature (mean  $T_a$ ) during the growing season months. . The colour indicates the density of data**  
 334 **points. For plotting (b), (c) and (d), only 10 percent random samples of the whole dataset are utilised.**

335 We use a random forest model to understand the spatial variability in the relevance of SSM versus TWS for NIRv. The model  
 336 was trained with 15 climatic, vegetation, and topographic predictors against the target variable which is the difference of the  
 337 partial correlations of NIRv with SSM and TWS during growing season-months ( $R^2 = 0.59$ , see **methods section 2.2.3**). The  
 338 mean absolute SHAP value plot shows that the tree cover and the climate variables (mean and standard deviation of  $T_a$ ) are  
 339 most important variables for explaining the spatial variability in the relative importance of SSM vs. TWS for vegetation

340 functioning (**Figure 4a**). This overall highlights that the relative importance of SSM vs. TWS for the vegetation is broadly  
341 controlled by vegetation type, reflecting the local adaptation of ecosystem and climate, influencing water availability.(Stocker  
342 et al., 2023).

343 Tree cover fraction is an important factor in determining the relevance of SSM and TWS for vegetation functioning (**Figure**  
344 **4c**). Regions with a high tree cover are more dependent on TWS, as trees generally have deeper root systems that allow them  
345 to adjust water uptake between different depths (Tao et al., 2021). Grasslands on the other hand have shallow roots that are  
346 more susceptible to surface soil moisture variations (Yang et al., 2014).

347  
348 Similarly, the relative importance of SSM and TWS varies non-linearly with the mean growing season temperature (**Figure**  
349 **4b**). TWS tends to be more crucial for vegetation functioning in areas with low (approximately below 20°C) or high (above  
350 27°C) growing season temperatures, while SSM has greater importance in regions with moderate growing season air  
351 temperatures. One possible explanation for this trend is that high temperatures induce a strong atmospheric water demand that  
352 dries near-surface soil layers, which leads vegetation to increase water extraction from deep soils. This observation is further  
353 underscored by the analogous pattern observed in the SHAP dependence plot for vpd, which accentuates atmospheric water  
354 demand (**Figure S8**). In contrast, SSM is more available during growing season months characterised by moderate  
355 temperatures. We hypothesize that the regions that experience relatively cold growing season temperatures exhibit stronger  
356 temperature and weather variability that may contribute to longer dry periods and, thus, emphasises the importance of deeper  
357 soil moisture for vegetation functioning. However, it should be noted that our findings regarding the relevance of TWS at high  
358 temperatures must be interpreted with caution due to the exclusion of most tropical forest regions from our analysis (**Figure**  
359 **S7**). As a result, most warm regions are dry, and there are only a few hot and wet regions included in our training data.

360  
361  
362 Not only the mean of the growing season temperature, but also its variability is crucial for explaining the significance of SSM  
363 and TWS for vegetation functioning (**Figure 4d**). A higher temporal variability in temperature increases the importance of  
364 TWS for vegetation. This is because atmospheric water demand scales with temperature. Hence, higher variability in  
365 temperature implies more peaks in related atmospheric water demand which is a stronger incentive for plants to access deeper  
366 water storages which are more often available to meet the vegetation's transpiration demand.

367  
368 **Figure S8** illustrates the effect of the other six important predictors on the model output. Apart from climatological parameters  
369 (mean P, mean vpd, variability in  $R_n$ , and aridity index), elevation and slope explain part of the variability in the relevance of  
370 SSM vs. TWS for NIRv. Although the reasons for increasing relevance of TWS for vegetation functioning at higher elevation  
371 remain unclear, it may be due to elevation's strong correlation with other climatic variables such as  $T_a$  and P.

372



373 Several local studies identified other relevant factors that determine root water uptake depth such as forest stand age and tree  
374 height, competition, root hydraulic architecture, and tree species (Zhu et al., 2022; Quijano et al., 2012; Stahl et al., 2013,  
375 Gessler et al., 2021; Liu et al., 2021). For example, young trees more easily increase their root activity in the shallow or deep  
376 soil dependent on soil moisture than mature trees (Zhu et al., 2022; Drake et al., 2011). These variables were not included in  
377 our attribution analysis, because they are not available at global scale.

### 378 **3.4 Robustness Tests**

379 In the aforementioned analysis, we included grid cells exhibiting both positive partial correlations, whether significant or non-  
380 significant. Upon further examination, we specifically assessed the evolution of partial correlation between NIRv and water  
381 storages, considering only grid cells with significant partial correlation ( $p < 0.05$ ). The observed patterns along the aridity-tree  
382 cover gradient remained similar during growing season months. This suggests the robustness of our results to the choice of the  
383 statistical significance criterion, albeit with a substantial reduction in the number of globally available grid cells when  
384 considering only significant partial correlation (**Figure S9**).

385  
386 Furthermore, to ensure that our results are robust to variations in the threshold for Solar-Induced Fluorescence (SIF) used to  
387 define growing season months, we conducted additional analyses with a different SIF threshold. Instead of filtering out all  
388 months from 2007-2018 when the mean-monthly SIF value was below the threshold of  $0.2 \text{ mW/m}^2/\text{sr/nm}$ , we utilized a  
389 threshold of  $0.5 \text{ mW/m}^2/\text{sr/nm}$ . Elevating the SIF threshold implies the exclusion of additional months characterized by lower  
390 vegetation activity for the partial correlation analysis. However, it is essential to note that this threshold does not seem to affect  
391 the number of globally available grid cells during growing season months and hence patterns along AI-TC classes are similar.  
392 Instead, it specifically influences the selection of dry months and hence the number of grid cells available for the analysis  
393 during dry months. . Nevertheless, even with the elevated SIF threshold for defining growing season months, the observed  
394 patterns along aridity-tree cover (AI-TC) classes remain largely consistent with the results obtained in our main analyses  
395 (**Figure S10**).

396  
397 Although NIRv can largely reflect vegetation functioning (Badgley et al., 2017), we repeat our analysis with SIF, which is an  
398 alternative and independent indicator for vegetation functioning and shows a near-linear relationship with gross primary  
399 productivity at the ecosystem level (Guanter et al., 2012). However, SIF is only available at a coarse resolution of 0.5 degree.  
400 The partial correlations,  $r(\text{SIF} \sim \text{SSM})$  and  $r(\text{SIF} \sim \text{TWS})$  largely agree with the pattern of  $r(\text{NIRv} \sim \text{SSM})$  and  $r(\text{NIRv} \sim \text{TWS})$   
401 across varying aridity index and tree cover classes (**Figure S11**). This suggests that our overall conclusion on the relevance of  
402 SSM or TWS for vegetation functioning is robust across different indicators of vegetation productivity.

403 Additionally, we tested if our results are robust when the aridity index is calculated based on the FAO Penman-Monteith  
404 Reference Evapotranspiration equation, for which we applied aridity classification based on UNEP 1997 guidelines - Our  
405 results confirm the findings of Section 3.1 and Figure 2 that as aridity increases, the correlation of NIRv with Soil Surface

406 Moisture (SSM) and Total Water Storage (TWS) intensifies. Moreover, in hyper arid regions ( $AI < 0.03$ ) the correlation with  
407 TWS surpasses that with SSM (**Figure S12**). They also confirm that regions with higher tree Cover (TC) fraction correlates  
408 more strongly with TWS compared to SSM. Thus, the choice of aridity index formulation does not alter our main conclusions.  
409

#### 410 **4. Summary and Conclusions**

411 In this study we compare the relevance of near-surface soil moisture and of terrestrial water storage for vegetation functioning  
412 across the globe. We find that in semi-arid regions and regions with low tree cover, vegetation preferentially utilises the water  
413 from shallow soil, which is related to continuous availability of near-surface water availability and lack of deep rooting systems  
414 respectively. The stronger correlation of NIRv with SSM than TWS is supported by site-level studies that find a higher root  
415 water uptake of surface soil moisture (Brinkmann et al., 2019, Gessler et al., 2021, Deseano Diaz et al., 2023; Kulmatiski and  
416 Beard, 2013), also when deeper water is available. Some local studies however find a higher root water uptake from deeper  
417 layers (Zhu et al., 2022).

418  
419 By contrast, in mostly forested regions and in relatively dry climate regimes, the correlation with terrestrial water storage is  
420 comparable or higher than with near-surface soil moisture, indicating that trees and vegetation in arid regions use their deep  
421 root systems to access deeper soil moisture. Point-scale studies also found a different water uptake depth for trees and grasses  
422 in for example savanna ecosystems (Kulmatiski et al., 2010), and a different water uptake depth for tree species (Kahmen et  
423 al., 2022). Liu et al. (2021) showed for example that for a karst forest in Southwest China, evergreen species rely mostly on  
424 water sources from the 0-30 cm layer, while deciduous species extracted most water from the 30-70 cm layer.

425  
426 We also find that vegetation's preferential water uptake depth changes over time. During particularly dry months, the relative  
427 importance of terrestrial water storage is higher, highlighting the importance of deep water resources during periods of low  
428 soil water availability. This is in line with previous studies showing changes in vegetation's water uptake depth during drought  
429 periods at small spatial scales where accessing water in deeper soil layers helps plants to alleviate water stress and maintain  
430 transpiration (Migliavacca et al., 2009; Tao et al., 2021).

431  
432 Our global results are supported by site-scale studies that find that, during drought, the deeper roots play a more active role in  
433 water extraction (Stahl et al., 2013, Volkmann et al., 2016; Tao et al., 2021). In some studies however, the increase of deep  
434 water uptake is only relative: the absolute uptake of deep water does not increase, but the uptake of shallow water decreases  
435 (Brinkmann et al., 2019, Gessler et al., 2021, Rasmussen et al., 2020; Kühnhammer et al., 2023). This means that the uptake  
436 of deeper soil layers cannot compensate for the loss of water uptake from the dry topsoil. Contrary to trees, grasses do not shift

437 their uptake depth (Deseano Diaz et al., 2023), or even extract water from the most shallow soils (Prechsl et al., 2015,  
438 Kulmatiski and Beard, 2013).

439

440 Furthermore, we show that the spatial variability of the importance of near-surface soil moisture vs. terrestrial water storage  
441 for vegetation functioning is influenced by fraction of tree cover and mean and standard deviation of air temperature. This  
442 emphasises the role of climate in determining shallow vs. deep soil water resources, and the role of vegetation in adapting to  
443 different soil water availability patterns.

444

445 Vegetation functioning and soil water storages are generally coupled in both directions, i.e. while soil moisture availability  
446 affects vegetation functioning (positive coupling), this in turn also affects soil moisture through transpiration (negative  
447 coupling). As our study focuses on water-controlled vegetation we only consider positive couplings and filter out grid cells  
448 with negative correlations. Future research may consider the relevance of soil moisture across depths for the positive coupling  
449 regions.

450

451 Overall, our analysis illustrates that satellite-based data can be used for belowground analysis at large spatial scales thanks to  
452 the fact that satellite retrievals can assess soil water storage dynamics across depths and because vegetation in water-controlled  
453 areas can be used as an indicator of soil water dynamics. Such novel ways to improve our understanding of belowground water  
454 dynamics is necessary and valuable as respective in-situ observations are scarce and of limited representativeness for larger  
455 areas, particularly given the typical spatial heterogeneity of soils and vegetation. Our results can further inform a better  
456 representation of belowground processes in global models in order to support more accurate projections of future changes in  
457 climate, water resources, and ecosystem services.

## 458 **Data availability**

459 The monthly SIF data is available from [https://www.gfz-potsdam.de/sektion/fernerkundungund-](https://www.gfz-potsdam.de/sektion/fernerkundungund-geoinformatik/projekte/global-monitoring-of-vegetation-fluorescence-globfluo/daten)  
460 [geoinformatik/projekte/global-monitoring-of-vegetation-fluorescence-globfluo/daten](https://www.gfz-potsdam.de/sektion/fernerkundungund-geoinformatik/projekte/global-monitoring-of-vegetation-fluorescence-globfluo/daten). The NIRv was calculated from the red  
461 and near-infrared reflectance obtained from the MOD13C1 v006 product (<https://lpdaac.usgs.gov/products/mod13c1v061/>).  
462 The ESA-CCI soil moisture can be accessed through <https://esa-soilmoisture-cci.org/> and Terrestrial Water Storage Anomaly  
463 data can be accessed through [https://podaac.jpl.nasa.gov/dataset/TELLUS\\_GRACGRFO\\_MASCON\\_CRI\\_GRID\\_RL06\\_V2](https://podaac.jpl.nasa.gov/dataset/TELLUS_GRACGRFO_MASCON_CRI_GRID_RL06_V2).  
464 The ERA5 climate variables are available from <https://www.ecmwf.int/en/forecasts/datasets/reanalysis-datasets/era5> . Tree  
465 cover fraction data is available from the AVHRR vegetation continuous fields products  
466 <https://lpdaac.usgs.gov/products/vcf5kyrv001/>, land cover data is available from <https://www.esa-landcover-cci.org/>, and  
467 topographic data is available via <https://www.earthenv.org/topography>. Similarly, the irrigation fraction data could be accessed  
468 from <https://mygeohub.org/publications/8> .

469 **Competing Interests**

470 The contact author has declared that none of the authors has any competing interests.

471 **Acknowledgements**

472 The authors thank Ulrich Weber for help with obtaining and processing the data, Sujan Koirala for valuable scientific and  
473 technical support and the Hydrology–Biosphere–Climate Interactions group at the Max Planck Institute for Biogeochemistry  
474 for fruitful discussions. Prajwal Khanal, Anne Hoek van Dijke and Rene Orth acknowledge funding by the German Research  
475 Foundation (Emmy Noether grant no. 391059971).

476 **References**

- 477 Amatulli, G., Domisch, S., Tuanmu, M.-N., Parmentier, B., Ranipeta, A., Malczyk, J., and Jetz, W.: A suite of global, cross-  
478 scale topographic variables for environmental and biodiversity modeling, *Sci Data*, 5, 180040,  
479 <https://doi.org/10.1038/sdata.2018.40>, 2018.
- 480 Badgley, G., Field, C. B., and Berry, J. A.: Canopy near-infrared reflectance and terrestrial photosynthesis, *Sci. Adv.*, 3,  
481 e1602244, <https://doi.org/10.1126/sciadv.1602244>, 2017.
- 482 Breiman, L.: [No title found], *Machine Learning*, 45, 5–32, <https://doi.org/10.1023/A:1010933404324>, 2001.
- 483 Budyko, M. I.: *Climate and life*, Academic press, 1974.
- 484 Chen, T. and Guestrin, C.: XGBoost: A Scalable Tree Boosting System, in: *Proceedings of the 22nd ACM SIGKDD*  
485 *International Conference on Knowledge Discovery and Data Mining, KDD '16: The 22nd ACM SIGKDD International*  
486 *Conference on Knowledge Discovery and Data Mining, San Francisco California USA*, 785–794,  
487 <https://doi.org/10.1145/2939672.2939785>, 2016.
- 488 Denissen, J. M. C., Teuling, A. J., Pitman, A. J., Koirala, S., Migliavacca, M., Li, W., Reichstein, M., Winkler, A. J., Zhan,  
489 C., and Orth, R.: Widespread shift from ecosystem energy to water limitation with climate change, *Nature Climate Change*,  
490 12, 677–684, <https://doi.org/10.1038/s41558-022-01403-8>, 2022.
- 491 Dorigo, W., Wagner, W., Albergel, C., Albrecht, F., Balsamo, G., Brocca, L., Chung, D., Ertl, M., Forkel, M., Gruber, A.,  
492 Haas, E., Hamer, P. D., Hirschi, M., Ikonen, J., de Jeu, R., Kidd, R., Lahoz, W., Liu, Y. Y., Miralles, D., Mistelbauer, T.,  
493 Nicolai-Shaw, N., Parinussa, R., Pratola, C., Reimer, C., van der Schalie, R., Seneviratne, S. I., Smolander, T., and Lecomte,  
494 P.: ESA CCI Soil Moisture for improved Earth system understanding: State-of-the art and future directions, *Remote Sensing*  
495 *of Environment*, 203, 185–215, 2017.
- 496 Fan, Y., Miguez-Macho, G., Jobbágy, E. G., Jackson, R. B., and Otero-Casal, C.: Hydrologic regulation of plant rooting depth,  
497 *Proceedings of the National Academy of Sciences of the United States of America*, 114, 10572–10577,  
498 <https://doi.org/10.1073/pnas.1712381114>, 2017.
- 499 Feldman, A. F., Short Gianotti, D. J., Dong, J., Akbar, R., Crow, W. T., McColl, K. A., Konings, A. G., Nippert, J. B., Tumber-  
500 Dávila, S. J., Holbrook, N. M., Rockwell, F. E., Scott, R. L., Reichle, R. H., Chatterjee, A., Joiner, J., Poulter, B., and Entekhabi,

- 501 D.: Remotely Sensed Soil Moisture Can Capture Dynamics Relevant to Plant Water Uptake, *Water Resources Research*, 59,  
502 e2022WR033814, <https://doi.org/10.1029/2022WR033814>, 2023.
- 503 Guanter, L., Frankenberg, C., Dudhia, A., Lewis, P. E., Gómez-Dans, J., Kuze, A., Suto, H., and Grainger, R. G.: Retrieval  
504 and global assessment of terrestrial chlorophyll fluorescence from GOSAT space measurements, *Remote Sensing of*  
505 *Environment*, 121, 236–251, <https://doi.org/10.1016/j.rse.2012.02.006>, 2012.
- 506 Hansen, Matthew and Song, Xiao-Peng: Vegetation Continuous Fields (VCF) Yearly Global 0.05 Deg,  
507 <https://doi.org/10.5067/MEASURES/VCF/VCF5KYR.001>, 2018.
- 508 Hersbach, H., Bell, B., Berrisford, P., Hirahara, S., Horányi, A., Muñoz-Sabater, J., Nicolas, J., Peubey, C., Radu, R., Schepers,  
509 D., Simmons, A., Soci, C., Abdalla, S., Abellan, X., Balsamo, G., Bechtold, P., Biavati, G., Bidlot, J., Bonavita, M., De Chiara,  
510 G., Dahlgren, P., Dee, D., Diamantakis, M., Dragani, R., Flemming, J., Forbes, R., Fuentes, M., Geer, A., Haimberger, L.,  
511 Healy, S., Hogan, R. J., Hólm, E., Janisková, M., Keeley, S., Laloyaux, P., Lopez, P., Lupu, C., Radnoti, G., de Rosnay, P.,  
512 Rozum, I., Vamborg, F., Villaume, S., and Thépaut, J.-N.: The ERA5 global reanalysis, *Quarterly Journal of the Royal*  
513 *Meteorological Society*, 146, 1999–2049, <https://doi.org/10.1002/qj.3803>, 2020.
- 514 Humphrey, V., Zscheischler, J., Ciais, P., Gudmundsson, L., Sitch, S., and Seneviratne, S. I.: Sensitivity of atmospheric CO<sub>2</sub>  
515 growth rate to observed changes in terrestrial water storage, *Nature*, 560, 628–631, [https://doi.org/10.1038/s41586-018-0424-](https://doi.org/10.1038/s41586-018-0424-4)  
516 [4](https://doi.org/10.1038/s41586-018-0424-4), 2018.
- 517 Keenan, T. F. and Williams, C. A.: The Terrestrial Carbon Sink, *Annual Review of Environment and Resources*, 43, 219–243,  
518 <https://doi.org/10.1146/annurev-environ-102017-030204>, 2018.
- 519 Köhler, P., Guanter, L., and Joiner, J.: A linear method for the retrieval of sun-induced chlorophyll fluorescence from GOME-  
520 2 and SCIAMACHY data, *Atmos. Meas. Tech.*, 8, 2589–2608, <https://doi.org/10.5194/amt-8-2589-2015>, 2015.
- 521 Koster, R. D., Guo, Z., Yang, R., Dirmeyer, P. A., Mitchell, K., and Puma, M. J.: On the nature of soil moisture in land surface  
522 models, *Journal of Climate*, 22, 4322–4335, <https://doi.org/10.1175/2009JCLI2832.1>, 2009.
- 523 Landerer, F. W. and Swenson, S. C.: Accuracy of scaled GRACE terrestrial water storage estimates, *Water Resources*  
524 *Research*, 48, <https://doi.org/10.1029/2011WR011453>, 2012.
- 525 Li, W., Migliavacca, M., Forkel, M., Walther, S., Reichstein, M., and Orth, R.: Revisiting Global Vegetation Controls Using  
526 Multi-Layer Soil Moisture, *Geophysical Research Letters*, 48, <https://doi.org/10.1029/2021GL092856>, 2021.
- 527 Li, W., Migliavacca, M., Forkel, M., Denissen, J. M. C., Reichstein, M., Yang, H., Duveiller, G., Weber, U., and Orth, R.:  
528 Widespread increasing vegetation sensitivity to soil moisture, *Nature Communications*, 13, 3959,  
529 <https://doi.org/10.1038/s41467-022-31667-9>, 2022.
- 530 Lundberg, S. M., Erion, G., Chen, H., DeGrave, A., Prutkin, J. M., Nair, B., Katz, R., Himmelfarb, J., Bansal, N., and Lee, S.-  
531 I.: From local explanations to global understanding with explainable AI for trees, *Nat Mach Intell*, 2, 56–67,  
532 <https://doi.org/10.1038/s42256-019-0138-9>, 2020.
- 533 Migliavacca, M., Meroni, M., Manca, G., Matteucci, G., Montagnani, L., Grassi, G., Zenone, T., Teobaldelli, M., Goded, I.,  
534 Colombo, R., and Seufert, G.: Seasonal and interannual patterns of carbon and water fluxes of a poplar plantation under  
535 peculiar eco-climatic conditions, *Agricultural and Forest Meteorology*, 149, 1460–1476,  
536 <https://doi.org/10.1016/j.agrformet.2009.04.003>, 2009.

- 537 Miguez-Macho, G. and Fan, Y.: Spatiotemporal origin of soil water taken up by vegetation, *Nature*, 598, 624–628,  
538 <https://doi.org/10.1038/s41586-021-03958-6>, 2021.
- 539 Mohammed, G. H., Colombo, R., Middleton, E. M., Rascher, U., van der Tol, C., Nedbal, L., Goulas, Y., Pérez-Priego, O.,  
540 Damm, A., Meroni, M., Joiner, J., Cogliati, S., Verhoef, W., Malenovsky, Z., Gastellu-Etchegorry, J.-P., Miller, J. R., Guanter,  
541 L., Moreno, J., Moya, I., Berry, J. A., Frankenberg, C., and Zarco-Tejada, P. J.: Remote sensing of solar-induced chlorophyll  
542 fluorescence (SIF) in vegetation: 50 years of progress, *Remote Sensing of Environment*, 231, 111177, 2019.
- 543 Ohta, T., Kotani, A., Iijima, Y., Maximov, T. C., Ito, S., Hanamura, M., Kononov, A. V., and Maximov, A. P.: Effects of  
544 waterlogging on water and carbon dioxide fluxes and environmental variables in a Siberian larch forest, 1998–2011,  
545 *Agricultural and Forest Meteorology*, 188, 64–75, <https://doi.org/10.1016/j.agrformet.2013.12.012>, 2014.
- 546 Orth, R.: When the Land Surface Shifts Gears, *AGU Advances*, 2, <https://doi.org/10.1029/2021AV000414>, 2021.
- 547 Qiu, R., Li, X., Han, G., Xiao, J., Ma, X., and Gong, W.: Monitoring drought impacts on crop productivity of the U.S. Midwest  
548 with solar-induced fluorescence: GOSIF outperforms GOME-2 SIF and MODIS NDVI, EVI, and NIRv, *Agricultural and  
549 Forest Meteorology*, 323, 109038, <https://doi.org/10.1016/j.agrformet.2022.109038>, 2022.
- 550 Reynolds, C. A., Jackson, T. J., and Rawls, W. J.: Estimating soil water-holding capacities by linking the Food and Agriculture  
551 Organization Soil map of the world with global pedon databases and continuous pedotransfer functions, *Water Resour. Res.*,  
552 36, 3653–3662, <https://doi.org/10.1029/2000WR900130>, 2000.
- 553 Schenk, H. J. and Jackson, R. B.: Rooting depths, lateral root spreads and below-ground/above-ground allometries of plants  
554 in water-limited ecosystems, *Journal of Ecology*, 90, 480–494, <https://doi.org/10.1046/j.1365-2745.2002.00682.x>, 2002.
- 555 Seneviratne, S. I., Corti, T., Davin, E. L., Hirschi, M., Jaeger, E. B., Lehner, I., Orlowsky, B., and Teuling, A. J.: Investigating  
556 soil moisture-climate interactions in a changing climate: A review, , 99, 125–161,  
557 <https://doi.org/10.1016/j.earscirev.2010.02.004>, 2010.
- 558 Siebert, S., Kumm, M., Porkka, M., Döll, P., Ramankutty, N., and Scanlon, B.: Historical Irrigation Dataset (HID),  
559 <https://doi.org/10.13019/M20599>, 2015.
- 560 Stocker, B. D., Tumber-Dávila, S. J., Konings, A. G., Anderson, M. C., Hain, C., and Jackson, R. B.: Global patterns of water  
561 storage in the rooting zones of vegetation, *Nat. Geosci.*, 16, 250–256, <https://doi.org/10.1038/s41561-023-01125-2>, 2023.
- 562 Tao, Z., Neil, E., and Si, B.: Determining deep root water uptake patterns with tree age in the Chinese loess area, *Agricultural  
563 Water Management*, 249, 106810, 2021.
- 564 Teuling, A. J., Hirschi, M., Ohmura, A., Wild, M., Reichstein, M., Ciais, P., Buchmann, N., Ammann, C., Montagnani, L.,  
565 Richardson, A. D., Wohlfahrt, G., and Seneviratne, S. I.: A regional perspective on trends in continental evaporation,  
566 *Geophysical Research Letters*, 36, <https://doi.org/10.1029/2008GL036584>, 2009.
- 567 Watkins, M. M., Wiese, D. N., Yuan, D., Boening, C., and Landerer, F. W.: Improved methods for observing Earth’s time  
568 variable mass distribution with GRACE using spherical cap mascons, *JGR Solid Earth*, 120, 2648–2671,  
569 <https://doi.org/10.1002/2014JB011547>, 2015.
- 570 Xie, X., He, B., Guo, L., Miao, C., and Zhang, Y.: Detecting hotspots of interactions between vegetation greenness and  
571 terrestrial water storage using satellite observations, *Remote Sensing of Environment*, 231, 111259, 2019.

572 Yang, Y., Long, D., Guan, H., Scanlon, B. R., Simmons, C. T., Jiang, L., and Xu, X.: GRACE satellite observed hydrological  
573 controls on interannual and seasonal variability in surface greenness over mainland Australia, *Journal of Geophysical*  
574 *Research: Biogeosciences*, 119, 2245–2260, <https://doi.org/10.1002/2014JG002670>, 2014.

575 Zomer, R. J., Xu, J., and Trabucco, A.: Version 3 of the Global Aridity Index and Potential Evapotranspiration Database, *Sci*  
576 *Data*, 9, 409, <https://doi.org/10.1038/s41597-022-01493-1>, 2022.

577

578

579

580